

Direct Observation of Ligand Migration in the Reversible Addition of Trimethylphosphine to 1,2-Mo₂(CH₂Ph)₂(O-*i*-Pr)₄ and Structural Characterization of (PMe₃)(PhCH₂)₂(*i*-PrO)Mo≡Mo(O-*i*-Pr)₃ and 1,2-Mo₂(CH₂Ph)₂(O-*i*-Pr)₄(dmpm), Where dmpm = Bis(dimethylphosphino)methane

Malcolm H. Chisholm,* Kirsten Folting, John C. Huffman, Keith S. Kramer, and Robert J. Tatz

Department of Chemistry and Molecular Structure Center, Indiana University, Bloomington, Indiana 47405

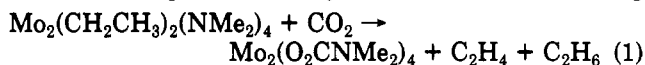
Received May 6, 1992

Addition of PMe₃ (1–2 equiv) to hydrocarbon solutions of 1,2-Mo₂(CH₂Ph)₂(O-*i*-Pr)₄ (I) at 22 °C leads to an equilibrium mixture of I, free PMe₃, and (PMe₃)(PhCH₂)₂(*i*-PrO)Mo≡Mo(O-*i*-Pr)₃ (II). Compound II is an orange crystalline solid that loses PMe₃ upon heating in vacuo (slowly at room temperature and rapidly at +50 °C) with the regeneration of I. Addition of 2 equiv of PMe₃ to I in toluene-*d*₈ at –80 °C yields a bisphosphine adduct (PMe₃)(PhCH₂)₂(*i*-PrO)₂Mo≡Mo(O-*i*-Pr)₂(CH₂Ph)(PMe₃) that yields II upon warming to +20 °C by way of an intermediate. When the solution is cooled, an unsymmetrical bisphosphine adduct (PMe₃)(PhCH₂)₂(*i*-PrO)Mo≡Mo(O-*i*-Pr)₃(PMe₃) is formed at –80 °C. The latter forms II reversibly by PMe₃ loss upon warming. Addition of dmpm to I in hexane or toluene (at –60 °C) yields 1,2-Mo₂(CH₂Ph)₂(O-*i*-Pr)₄(μ-dmpm) (III), where dmpm = bis(dimethylphosphino)methane. Compound III was isolated at –25 °C by crystallization. In toluene-*d*₈ and at room temperature, the ¹H and ³¹P NMR spectra indicate the presence of an isomeric form of III, (η¹-dmpm)(PhCH₂)₂(*i*-PrO)Mo≡Mo(O-*i*-Pr)₃. Addition of dmpe (1 equiv) to hydrocarbon solutions of I yields an insoluble crystalline material Mo₂(CH₂Ph)₂(O-*i*-Pr)₄(dmpe) (IV), where dmpe = 1,2-bis(dimethylphosphino)ethane. Compound IV is sparingly soluble in tetrahydrofuran and upon photolysis in the presence of additional dmpe compound IV is converted to Mo₂(O-*i*-Pr)₄(dmpe)₂ and bibenzyl. Crystal data: for II at –159 °C *a* = 16.779 (3) Å, *b* = 10.104 (1) Å, *c* = 19.555 (4) Å, β = 90.59 (10)°, *Z* = 4, *d*_{calcd} = 1.38 g cm^{–3} and space group *P*2₁/*c*; for III at –168 °C *a* = 14.952 (2) Å, *b* = 29.252 (4) Å, *c* = 17.637 (2) Å, β = 111.05 (1)°, *Z* = 8, *d*_{calcd} = 1.38 g cm^{–3}, and space group *P*2₁/*n*.

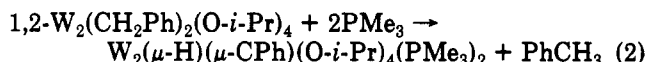
Introduction

In dinuclear and polynuclear chemistry (i.e. cluster chemistry), one of the most elementary and fundamentally important questions concerns which reactions occur at a single metal site versus those that occur across two or more metal atoms.^{1,2} For example, when a dinuclear or polynuclear complex represented by L_{*n*}M_{*x*} is labile to oxidative addition of a substrate X–Y to yield L_{*n*}M_{*x*}(X)(Y), one must ask: how does the addition step occur? For elimination of X–Y from L_{*n*}M_{*x*}(X)(Y), the question is similarly raised.

In our development of the dinuclear chemistry of molybdenum and tungsten, we have found several examples of elimination reactions (and addition reactions) that we have shown to be unimolecular in the M₂ complex by labeling studies, e.g. the elimination of ethylene and ethane as shown in eq 1.³ Similarly, in the reactions involving



1,2-W₂(CH₂Ph)₂(O-*i*-Pr)₄ and Lewis bases such as PMe₃, toluene is eliminated with the formation of hydrido-benzylidyne complexes, eq 2.⁴



In reactions such as those in (1) and (2) we must ask the question does elimination occur by C–H activation across the M–M bond or does alkyl group migration precede an elimination that occurs from one metal center? In this paper we describe reactions involving 1,2-Mo₂(CH₂Ph)₂(O-*i*-Pr)₄ and PMe₃ that provide the first examples of the direct observation of facile ligand exchange across the M–M triple bond in M⁶⁺-containing compounds.⁵ These results are particularly pertinent to studies of reaction 2 that are described in a following paper.

Results and Discussion

Synthesis. The addition of PMe₃ (2–3 equiv) to 1,2-Mo₂(CH₂Ph)₂(O-*i*-Pr)₄ (I) in a hydrocarbon solvent, typically hexane, yields Mo₂(CH₂Ph)₂(O-*i*-Pr)₄(PMe₃) (II). Crystals were obtained by cooling a concentrated solution of the mother liquor to –20 °C.

In an analogous manner, the addition of dmpm, bis(dimethylphosphino)methane, to a toluene or hexane solution of I yields Mo₂(CH₂Ph)₂(O-*i*-Pr)₄(dmpm) (III). The addition of dmpe, 1,2-bis(dimethylphosphino)ethane, to hydrocarbon solutions of I also yields a 1:1 adduct, Mo₂-

(1) For some examples of reactions involving alkyl migrations and reductive eliminations at dinuclear metal centers see: (a) Kellenberger, B.; Young, S. J.; Stille, J. K. *J. Am. Chem. Soc.* 1985, 107, 6105. (b) Ling, S. S. M.; Payne, N. C.; Puddephatt, R. *J. Organometallics* 1985, 4, 1546. (c) Arnold, D. R.; Bennett, M. A.; McLaughlin, G. M.; Robertson, G. B.; Whittaker, M. J. *J. Chem. Soc., Chem. Commun.* 1983, 1, 32. (d) Norton, J. R. *Acc. Chem. Res.* 1979, 12, 139. (e) Bergman, R. G. *Acc. Chem. Res.* 1980, 13, 113.

(2) There are numerous examples of ligand degradations at multinuclear metal centers wherein the cooperative effects of the metal atoms facilitate multicenter transformations: (a) Calvert, R. B.; Shapley, J. R. *J. Am. Chem. Soc.* 1978, 100, 7726. (b) Vahrenkamp, H. *Pure Appl. Chem.* 1991, 63, 643. (c) Hansert, B.; Tasi, M.; Tiripicchio, A.; Camellini, M. T.; Vahrenkamp, H.; *Organometallics* 1991, 10, 4070. (d) Adams, R. D. In *Metal–Metal Bonds and Clusters in Catalysis*; Fackler, J. P., Jr., Ed.; Texas A&M University Press: College Station, TX, 1989.

(3) Chetcuti, M. J.; Chisholm, M. H.; Folting, K.; Haitko, D. A.; Huffman, J. C. *J. Am. Chem. Soc.* 1982, 104, 2138.

(4) Chisholm, M. H.; Eichhorn, B. W.; Folting, K.; Huffman, T. C.; Kramer, K. S.; Streib, W. E. Results to be published.

(5) A preliminary account of some of these findings has appeared: Chisholm, M. H.; Huffman, J. C.; Tatz, R. J. *J. Am. Chem. Soc.* 1984, 106, 5385.

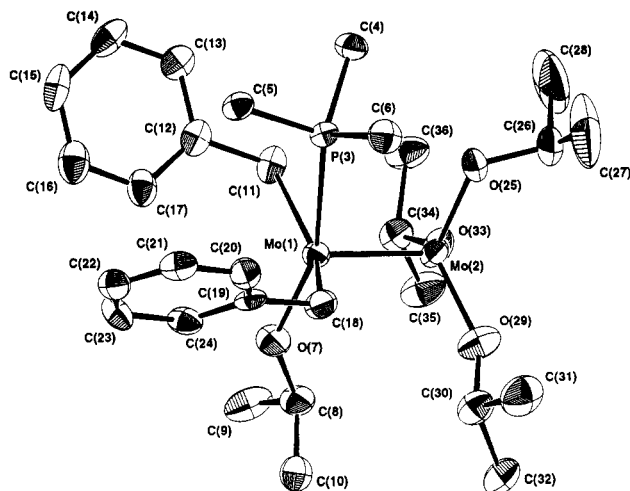
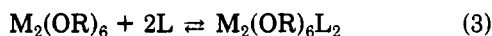


Figure 1. ORTEP drawing of the $\text{Mo}_2(\text{CH}_2\text{Ph})_2(\text{O}-i\text{-Pr})_4(\text{PMe}_3)$ (II) molecule showing the atom number scheme used in the tables. Atoms are drawn at the 50% probability level.

$(\text{CH}_2\text{Ph})_2(\text{O}-i\text{-Pr})_4(\text{dmpe})$ (IV), but, in contrast to the adducts II and III, compound IV is insoluble in hydrocarbon solvents and only sparingly soluble in tetrahydrofuran (THF). The insolubility of IV is somewhat surprising. Indeed, it is sufficiently surprising that we wonder whether or not compound IV is a simple dinuclear complex in the solid state. It is possible that the dmpe ligands bridge between dinuclear centers so as to yield a polymer.⁶ Although the reaction between I and dmpe in dilute solutions yielded large crystals of IV, the crystals appeared twinned by X-ray analysis. Regrettably, the molecular structure of IV remains unknown.

The compounds I–III are air-sensitive and must be handled in a dry and inert atmosphere (N_2). By contrast, crystals of IV are relatively air-stable (at least for periods of a few days) and are even inert to the commonly reactive solvents ethanol and acetone in which IV is insoluble.

Crystal and Molecular Structures. $\text{Mo}_2(\text{CH}_2\text{Ph})_2(\text{O}-i\text{-Pr})_4(\text{PMe}_3)$ (II). An ORTEP view of the molecular structure of compound II is shown in Figure 1, and a view looking down the M–M bond is given in Figure 2. One molybdenum atom is coordinated to four ligands, one *O-i-Pr*, one PMe_3 , and two benzyl groups and the other is trigonally ligated by three *O-i-Pr* ligands. The molecular structure of II provides a rare example of an unbridged Mo–Mo triple bond uniting 3- and 4-coordinated metal atoms.⁷ In general, the metal atoms share the same coordination number be it 3, 4, 5, or 6 as in $\text{M}_2(\text{OR})_6$, $\text{Mo}(\text{OR})_6\text{L}_2$, $\text{W}_2\text{Me}_2(\text{O}_2\text{CNEt}_2)_4$, or $\text{W}_2(\text{O}_2\text{C}-t\text{-Bu})_6$, respectively.⁷ The only other structurally characterized example of an unbridged M–M triple bond having 3- and 4-coordinate metal atoms is seen in $\text{W}_2(\text{Ar})_2(\text{O}-i\text{-Pr})_4(\text{HNMe}_2)$, where Ar = phenyl or *p*-tolyl, which, rather interestingly, has a 1,2-diaryl substitution pattern in contrast to II.⁸ Although the isolation of $(\text{M}\equiv\text{M})^{6+}$ -containing compounds with seven ligands is rare, they are presumably common intermediates in the facile reversible reactions of the general type shown in eq 3.⁹



L = Lewis base such as py, PR_3 , etc.

(6) Kerby, M. C.; Eichhorn, B. W.; Crieghton, J. A.; Vollhardt, K. P. C. *Inorg. Chem.* 1990, 29, 1319.

(7) Chisholm, M. H. *Acc. Chem. Res.* 1990, 23, 419.

(8) Chisholm, M. H.; Eichhorn, B. W.; Folting, K.; Huffman, J. C.; Tatz, R. J. *Organometallics* 1986, 5, 1599.

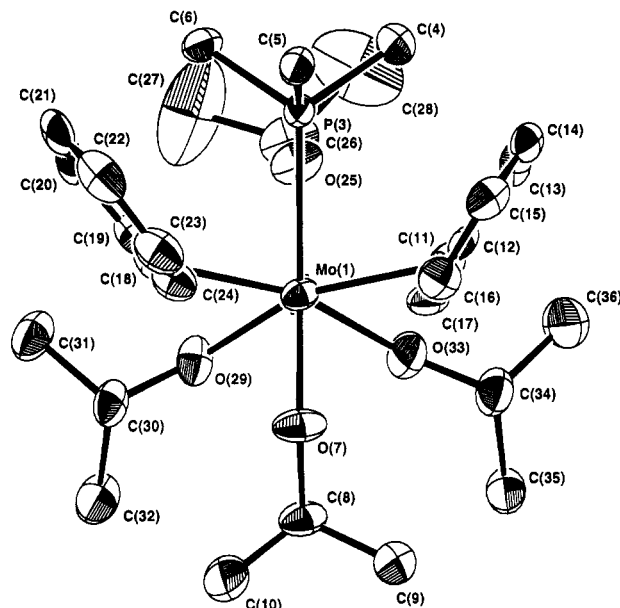
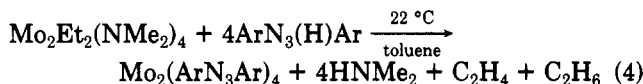


Figure 2. ORTEP drawing of the $\text{Mo}_2(\text{CH}_2\text{Ph})_2(\text{O}-i\text{-Pr})_4(\text{PMe}_3)$ (II) molecule looking down the Mo–Mo bond axis.

The Mo–Mo distance in II is 2.253 (1) Å, typical of a Mo–Mo distance in a $(\text{Mo}\equiv\text{Mo})^{6+}$ -containing compound.^{7,10} The Mo–O distances associated with the Mo(OR)₃ moiety, 1.89 (1) Å (average), are as seen in $\text{M}_2(\text{OR})_6$ compounds, and the Mo(1)–O distance, 1.92 (1) Å, is somewhat longer, as expected when there are four groups at the Mo center.⁹ The Mo–C distances, 2.214 (6) and 2.218 (6) Å, are as expected, and may be compared with the Mo–C₂H₅ distance in 1,2- $\text{Mo}_2\text{Et}_2(\text{NMe}_2)_2(\text{ArN}_3\text{Ar})_2$, 2.21 (1) Å (average), a compound that has been structurally characterized and shown to be an intermediate in the formation of $\text{Mo}_2(\text{ArN}_3\text{Ar})_4$ during the reaction between $\text{Mo}_2\text{Et}_2(\text{NMe}_2)_4$ and 1,3-diaryltriazines, eq 4.³



By taking the covalent radius for C_{sp^3} to be 0.77 Å, we can estimate the radius of the 4-coordinate Mo atom in II to be 1.44 Å and the covalent radius for phosphorus to be 1.05 Å. This leads us to predict a Mo– PMe_3 distance of 2.49 Å which is roughly 0.1 Å less than the observed distance. Thus, the Mo–P distance of 2.581 (2) Å is consistent with a relatively weak and labile bond. A similar expectation can be seen by inspection of the angles of the MoC₂OP moiety. The C–Mo–P angles, 78.1 (1) and 77.7 (1)°, are smaller than the C–Mo–O angles, 97.5 (1)°. We can view the Mo($\text{CH}_2\text{Ph})_2(\text{O}-i\text{-Pr})(\text{PMe}_3)$ moiety as a 4-coordinate metal center wherein one bond, the Mo– PMe_3 bond, is about to be broken or, alternatively, as a trigonal Mo($\text{CH}_2\text{Ph})_2(\text{O}-i\text{-Pr})$ center that has just formed a weak bond to the Lewis base PMe_3 .

$\text{Mo}_2(\text{CH}_2\text{Ph})_2(\text{O}-i\text{-Pr})_4(\text{dmpm})$ (III). A view of the molecular structure of III looking perpendicular to the Mo–Mo bond is shown in Figure 3, and a view down the Mo–Mo bond is given in Figure 4. In the space group $P2_1/n$, there are two independent molecules in the unit cell, differing little in their structural parameters. The basic description of the molecule is one wherein two 4-coordinate Mo atoms are united by a Mo–Mo triple bond

(9) Chisholm, M. H. *Polyhedron* 1983, 2, 681.

(10) Cotton, F. A.; Walton, R. A. *Multiple Bonds Between Metal Atoms*; Wiley: New York, 1982.

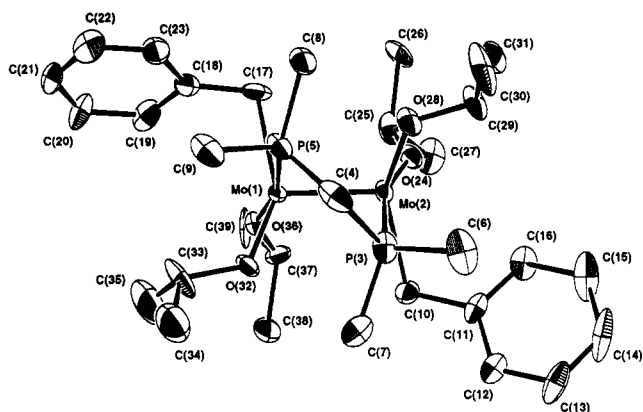


Figure 3. ORTEP drawing of the $\text{Mo}_2(\text{CH}_2\text{Ph})_2(\text{O-}i\text{-Pr})_4$ (dmpm) (III) molecule showing the atom number scheme used in the tables. The atoms are drawn at the 50% probability level.

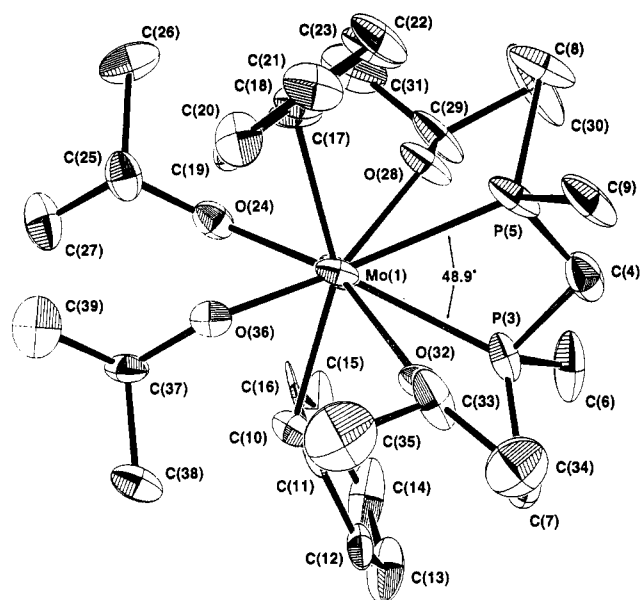


Figure 4. ORTEP drawing of the $\text{Mo}_2(\text{CH}_2\text{Ph})_2(\text{O-}i\text{-Pr})_4$ (dmpm) (III) molecule looking down the Mo-Mo bond axis showing the staggered conformation of ligands. The P-Mo-Mo-P torsional angle is included.

that is spanned by a bridging dmpm ligand. The presence of a $\sigma^2\pi^4$ cylindrical triple bond imposes no preference for an eclipsed structure, and unlike dmpm-bridged Mo-Mo quadruply bonded complexes,¹⁰ the structure of III is distinctly staggered. There is one benzyl ligand at each Mo atom and this is cis to the Mo-P bond. The Mo-P distances span the range 2.56 (1)–2.63 (1) Å, and again these may be viewed as somewhat long. The Mo-O distances fall into two sets spanning the range 1.91 and 1.98 Å with those trans to the Mo-C bond, 1.98 Å, consistent with the trans influence order $\text{PhCH}_2 \gtrsim \text{PMe}_3$.¹¹ The fact that in II the two PhCH_2 groups were mutually trans suggests an overall trans influence order of $\text{RO} > \text{PhCH}_2 > \text{PMe}_3$ for ligation to the $(\text{Mo}\equiv\text{Mo})^{6+}$ center. This is not what would be expected for binding to Pt(2+) but presumably the strong σ - and π -bonding involved in Mo-OR bonds switches the order of PhCH_2 and OR for a Mo(3+) center.

A summary of crystal data for compounds II and III is given in Table I. Selected bond distances and bond angles are given in Tables II and III.

Table I. Summary of Crystal Data^a

	II	III
empirical formula	$\text{Mo}_2\text{PO}_4\text{C}_{29}\text{H}_{51}$	$\text{C}_{31}\text{H}_{56}\text{Mo}_2\text{O}_4\text{P}_2$
color of cryst	black	red
cryst dims (mm)	$0.15 \times 0.15 \times 0.23$	$0.28 \times 0.28 \times 0.32$
space group	$P2_1/c$	$P2_1/n$
cell dims		
temp ($^\circ\text{C}$)	-159	-168
<i>a</i> (Å)	16.779 (3)	14.952 (2)
<i>b</i> (Å)	10.104 (1)	29.252 (4)
<i>c</i> (Å)	19.555 (4)	17.637 (2)
β (deg)	90.59 (1)	111.05 (1)
<i>Z</i> (molecules/cell)	4	8
vol (\AA^3)	3315.03	7199.33
calcd dens (g/cm^3)	1.376	1.378
wavelength (Å)	0.710 69	0.710 69
mol wt	686.57	746.61
linear abs coeff (cm^{-1})	8.137	7.970
detector to sample dist (cm)	22.5	22.5
sample to source dist (cm)	23.5	23.5
av ω scan width at half-height	0.25	0.25
scan speed (deg/min)	4.0	8.0
scan width (deg + dispersion)	2.0	1.4
individual bckgd (s)	8	4
aperture size (mm)	3.0×4.0	3.0×4.0
2θ range (deg)	6–45	6–45
total no. of refls colld	4823	18 281
no. of unique intns	4333	9462
no. with $F > 0.0$		7964
no. with $F > 3\sigma(R)$	3665	6231
$R(F)$	0.0375	0.0557
$R_w(F)$	0.0409	0.0560
goodness of fit for the last cycle	0.972	0.914
max δ/σ for last cycle	0.05	0.05

^a II = $\text{Mo}_2(\text{CH}_2\text{Ph})_2(\text{O-}i\text{-Pr})_4(\text{PMe}_3)$, III = $\text{Mo}_2(\text{CH}_2\text{Ph})_2(\text{O-}i\text{-Pr})_4(\text{dmpm})$.

Table II. Selected Bond Distances (Å) and Angles (deg) for the $\text{Mo}_2(\text{CH}_2\text{Ph})_2(\text{O-}i\text{-Pr})_4(\text{PMe}_3)$ Molecule

Mo(1)–Mo(2)	2.2350 (7)	Mo(1)–C(18)	2.218 (6)
Mo(1)–P(3)	2.5813 (15)	Mo(2)–O(25)	1.911 (4)
Mo(1)–O(7)	1.920 (4)	Mo(2)–O(29)	1.881 (4)
Mo(1)–C(11)	2.214 (6)	Mo(2)–O(33)	1.874 (4)
Mo(2)–Mo(1)–P(3)	94.65 (4)	O(25)–Mo(2)–O(29)	112.60 (17)
Mo(2)–Mo(1)–O(7)	106.55 (11)	O(25)–Mo(2)–O(33)	111.93 (18)
Mo(2)–Mo(1)–C(11)	101.89 (16)	O(29)–Mo(2)–O(33)	110.43 (18)
Mo(2)–Mo(1)–C(18)	100.76 (15)	Mo(1)–P(3)–C(4)	118.40 (24)
P(3)–Mo(1)–O(7)	158.80 (12)	Mo(1)–P(3)–C(5)	114.69 (22)
P(3)–Mo(1)–C(11)	78.10 (17)	Mo(1)–P(3)–C(6)	118.28 (22)
P(3)–Mo(1)–C(18)	77.71 (16)	C(4)–P(3)–C(5)	101.0 (3)
O(7)–Mo(1)–C(11)	97.49 (21)	Mo(1)–O(7)–C(8)	137.5 (4)
O(7)–Mo(1)–C(18)	97.49 (21)	Mo(2)–O(25)–C(26)	118.1 (4)
C(11)–Mo(1)–C(18)	147.93 (21)	Mo(2)–O(29)–C(30)	145.1 (3)
Mo(1)–Mo(2)–O(25)	105.46 (11)	Mo(2)–O(33)–C(34)	148.5 (4)
Mo(1)–Mo(2)–O(29)	107.08 (12)	Mo(1)–C(11)–C(12)	113.7 (4)
Mo(1)–Mo(2)–O(33)	109.06 (14)	Mo(1)–C(18)–C(19)	115.1 (4)

NMR Studies of the Solution Behavior of $\text{Mo}_2(\text{CH}_2\text{Ph})_2(\text{O-}i\text{-Pr})_4(\text{PMe}_3)$ (II) and the Reaction between $\text{Mo}_2(\text{CH}_2\text{Ph})_2(\text{O-}i\text{-Pr})_4$ (I) and PMe_3 . The reaction between $1,2\text{-Mo}_2(\text{CH}_2\text{Ph})_2(\text{O-}i\text{-Pr})_4$ (I) and PMe_3 (1–5 equiv) has been studied by variable-temperature ^1H and ^{31}P NMR spectroscopy and leads to some fascinating insights into the various equilibria that they exhibit, as shown in Scheme I.

If the addition of PMe_3 (2.5 equiv) is made at low temperatures, ca. -78°C , then the ^{31}P NMR spectrum reveals a signal at ca. $\delta -2.8$ at -80°C that can be assigned to a bisphosphine adduct. See Figure 5. We propose that the kinetic product of the low-temperature addition of PMe_3 is the symmetrical adduct $1,2\text{-Mo}_2(\text{CH}_2\text{Ph})_2(\text{O-}i\text{-Pr})_4(\text{PMe}_3)_2$, an analogue of $\text{W}_2(\text{O-}i\text{-Pr})_6(\text{PMe}_3)_2$.⁹ For brevity we shall refer to this as $[\text{M}_2]\text{L}_2$ where one PMe_3 coordinates to each $\text{Mo}(\text{CH}_2\text{Ph})(\text{O-}i\text{-Pr})_2$ center and there is an un-

(11) Appleton, T. G.; Clark, H. C.; Manzer, L. E. *Coord. Chem. Rev.* 1972, 10, 353.

Scheme I. Proposed Reaction Sequence Showing the Facile 1,2- to 1,1-Dialkyl Ditungsten Isomerizations That Occur in the Presence of PMe_3

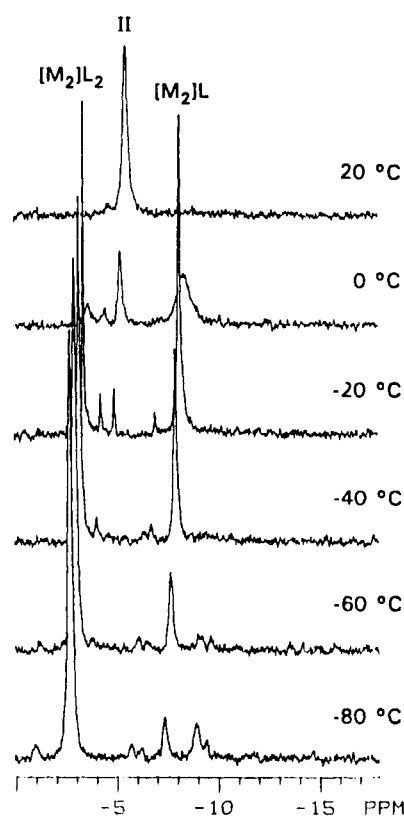
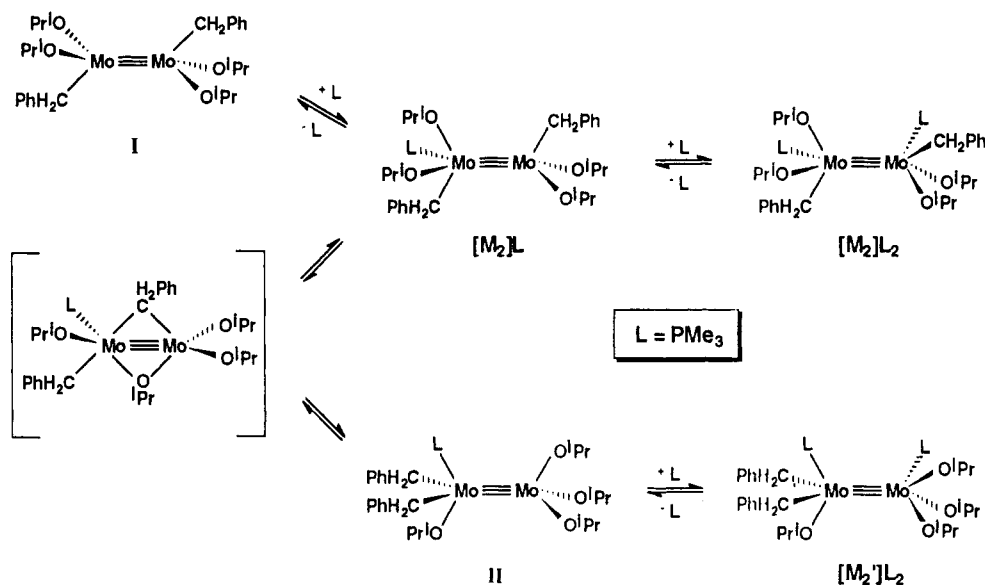


Figure 5. $^{31}\text{P}\{^1\text{H}\}$ NMR spectra for the temperature-dependent reaction of I and PMe_3 (2.5 equiv). The ^{31}P signal for free PMe_3 at $\delta -61$ is not shown.

bridged $\text{Mo}\equiv\text{Mo}$ bond. When the sample is warmed to -40°C , the signal assignable to $[\text{M}_2]\text{L}_2$ ($\delta -2.8$) decreases in intensity, the signal assignable to free PMe_3 at $\delta -61$ increases in intensity, and a new signal at ca. $\delta -8.0$ appears (Figure 5). From the increase in the intensity of the PMe_3 signal and the decrease in the intensity of the signal assigned to $[\text{M}_2]\text{L}_2$ ($\delta -2.8$) and the increase in signal intensity of the new resonance at ca. $\delta -8.0$, we assign the latter to a monophosphine adduct $[\text{M}_2]\text{L}$. From the appearance of the signals, which are broad, it is evident that there is an exchange process that is scrambling the PMe_3 ligands. We ascribe this to the simple equilibrium reaction

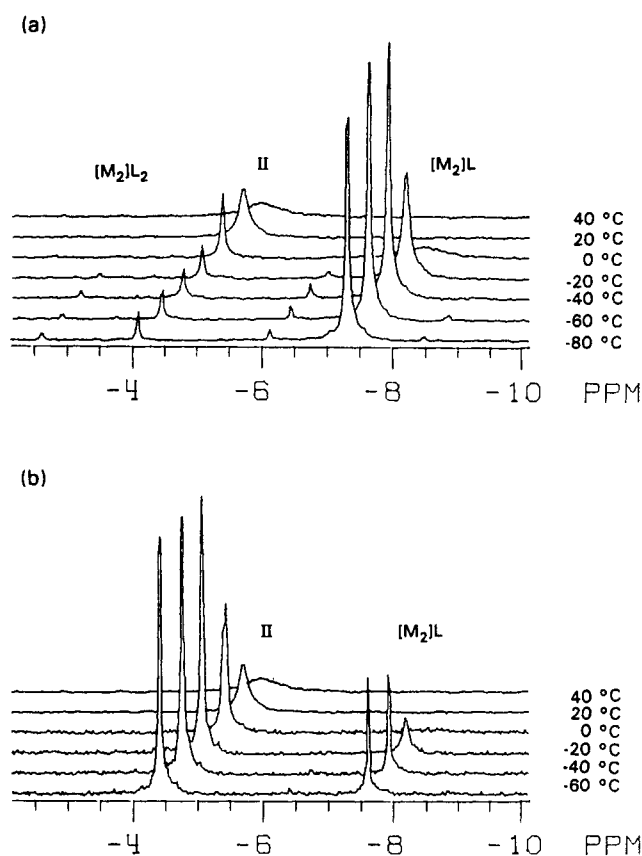
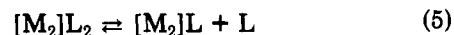


Figure 6. $^{31}\text{P}\{^1\text{H}\}$ NMR spectra for (a) the temperature-dependent reaction of I and PMe_3 (1 equiv) and (b) the equilibrium between II and $[\text{M}_2]\text{L}$.

shown in eq 5. Reaction 5 is fully reversible in the temperature range -80 to -40°C in toluene- d_8 .



If only 1 equiv of PMe_3 is added to I at -78°C , the ^{31}P spectrum at -80°C shows that $[\text{M}_2]\text{L}$ is the major species present. See Figure 6a. Only a very small amount of $[\text{M}_2]\text{L}_2$ can be detected by ^{31}P NMR spectroscopy. The equilibrium 5 is therefore chemically rapid in the temperature range -80 to -40°C , although it is slow on the NMR time scale.

Table III. Selected Bond Distances (Å) and Angles (deg) for the $\text{Mo}_2(\text{CH}_2\text{Ph})_2(\text{OR})_4(\text{dmpm})$ Molecule

Mo(1)A-Mo(2)A	2.2540 (11)	Mo(1)B-Mo(2)B	2.2525 (12)
Mo(1)A-P(5)A	2.628 (3)	Mo(1)B-P(5)B	2.6038 (28)
Mo(1)A-O(32)A	1.696 (6)	Mo(1)B-O(32)B	1.982 (6)
Mo(1)A-O(36)A	1.911 (6)	Mo(1)B-O(36)B	1.910 (6)
Mo(1)A-C(17)A	2.196 (9)	Mo(1)B-C(17)B	2.202 (9)
Mo(2)A-P(3)A	2.556 (3)	Mo(2)B-P(3)B	2.570 (3)
Mo(2)A-O(24)A	1.923 (6)	Mo(2)B-O(24)B	1.923 (6)
Mo(2)A-O(28)A	1.966 (6)	Mo(2)B-O(28)B	1.961 (6)
Mo(2)A-C(10)A	2.208 (9)	Mo(2)B-C(10)B	2.220 (9)
Mo(2)A-Mo(1)A-P(5)A	88.26 (7)	O(32)B-Mo(1)B-C(17)B	140.7 (3)
Mo(2)A-Mo(1)A-O(32)A	109.78 (18)	O(36)B-Mo(1)B-C(17)B	92.3 (3)
Mo(2)A-Mo(1)A-O(36)A	105.36 (17)	Mo(1)B-Mo(2)B-P(3)B	89.34 (8)
Mo(2)A-Mo(1)A-C(17)A	100.14 (27)	Mo(1)B-Mo(2)B-O(24)B	107.53 (18)
P(5)A-Mo(1)A-O(32)A	76.05 (19)	Mo(1)B-Mo(2)B-O(28)B	106.71 (20)
P(5)A-Mo(1)A-O(36)A	166.13 (18)	Mo(1)B-Mo(2)B-C(10)B	100.26 (25)
P(5)A-Mo(1)A-C(17)A	83.3 (3)	P(3)B-Mo(2)B-O(24)B	162.47 (19)
O(32)A-Mo(1)A-O(36)A	101.13 (25)	P(3)B-Mo(2)B-O(28)B	76.93 (20)
O(32)A-Mo(1)A-C(17)A	142.7 (3)	P(3)B-Mo(2)B-C(10)B	80.70 (25)
O(36)A-Mo(1)A-C(17)A	91.6 (3)	O(24)B-Mo(2)B-O(28)B	101.9 (3)
Mo(1)A-Mo(2)A-P(3)A	89.74 (7)	O(24)B-Mo(2)B-C(10)B	91.4 (3)
Mo(1)A-Mo(2)A-O(24)A	107.49 (18)	O(28)B-Mo(2)B-C(10)B	144.4 (3)
Mo(1)A-Mo(2)A-O(28)A	106.63 (19)	Mo(2)A-P(3)A-C(4)A	106.0 (4)
Mo(1)A-Mo(2)A-C(10)A	101.40 (24)	Mo(2)A-P(3)A-C(6)A	116.9 (4)
P(3)A-Mo(2)A-O(24)A	162.33 (19)	Mo(2)A-P(3)A-C(7)A	122.5 (3)
P(3)A-Mo(2)A-O(28)A	76.80 (22)	Mo(2)A-O(24)A-C(25)A	145.8 (6)
P(3)A-Mo(2)A-C(10)A	80.56 (26)	Mo(2)A-O(28)A-C(29)A	121.7 (5)
O(24)A-Mo(2)A-O(28)A	101.21 (28)	Mo(1)A-O(32)A-C(33)A	121.5 (6)
O(24)A-Mo(2)A-C(10)A	91.9 (3)	Mo(1)A-O(36)A-C(37)A	143.2 (5)
O(28)A-Mo(2)A-C(10)A	143.6 (3)	Mo(2)B-O(24)B-C(25)B	142.5 (5)
Mo(2)B-Mo(1)B-P(5)B	88.69 (8)	Mo(2)B-O(28)B-C(28)B	133.6 (9)
Mo(2)B-Mo(1)B-O(32)B	109.23 (19)	Mo(1)B-O(32)B-C(33)B	122.5 (6)
Mo(2)B-Mo(1)B-O(36)B	106.13 (18)	Mo(1)B-O(36)B-C(37)B	145.6 (6)
Mo(2)B-Mo(1)B-C(17)B	102.02 (26)	Mo(2)A-C(10)A-C(11)A	110.2 (6)
P(5)B-Mo(1)B-O(32)B	76.06 (19)	Mo(1)A-C(17)A-C(18)A	105.6 (6)
P(5)B-Mo(1)B-O(36)B	164.91 (19)	Mo(2)A-C(10)B-C(11)B	111.0 (6)
P(5)B-Mo(1)B-C(17)B	81.60 (28)	Mo(1)B-C(17)B-C(18)B	106.3 (6)
O(32)B-Mo(1)B-O(36)B	101.02 (26)		

As the temperature is raised above -40°C a new ^{31}P signal appears (ca. $\delta -4.8$) that can be assigned to the monophosphine complex II (Figure 6a). In the temperature range -20 to $+20^\circ\text{C}$, the monophosphine complex $[\text{M}_2]\text{L}$ is isomerized to II. The line broadening of the signals associated with $[\text{M}_2]\text{L}$ and PMe_3 indicates that they are in a relatively fast exchange (eq 5) while the ^{31}P signal assigned to II is in a slower exchange. These changes are shown in Figure 6a. However, when the temperature is raised to $+55^\circ\text{C}$, the ^{31}P signal of II decreases in intensity while that of free phosphine, $\delta -61$, increases further. In the temperature range $+20$ to $+55^\circ\text{C}$, the spectra reveal only the equilibrium between II and I and PMe_3 .

If a pure crystalline sample of II is dissolved in toluene- d_8 at -78°C , the low-temperature ^{31}P spectrum shows only the signal at $\delta -4.8$. At 22°C the ^{31}P NMR spectrum reveals that II and PMe_3 are present in solution. The ^1H NMR spectra in the range -35 to $+10^\circ\text{C}$ are as expected for II. There are two types of *O-i-Pr* ligands in the integral ratio 3:1, which is consistent with rapid rotation about the $\text{Mo}\equiv\text{Mo}$ bond in II. The methylene protons of the benzyl ligand appear as an ABX spin system where $\text{X} = ^{31}\text{P}$. When the temperature is raised to $+55^\circ\text{C}$, II is converted to I and free PMe_3 . Upon lowering of the temperature, II is reformed but, at low temperatures, the ^1H NMR spectra are complicated. In part this might be anticipated on the basis of restricted rotation about the $\text{M}\equiv\text{M}$ bond below -40°C . However, the ^{31}P NMR spectra at -20°C and below show that II and $[\text{M}_2]\text{L}$ are present in the approximate ratio 3:1, respectively. See Figure 6b.

In the presence of excess PMe_3 , compound II reacts to form a bisphosphine adduct that has signals at $\delta -2.6$ and -14.5 in the integral ratio 1:1. See Figure 7. We assign

these ^{31}P signals to the compound $(\text{PMe}_3)(\text{PhCH}_2)_2(i\text{-PrO})\text{Mo}\equiv\text{Mo}(\text{O-}i\text{-Pr})_3(\text{PMe}_3)$ which we abbreviate as $[\text{M}_2']\text{L}_2$. The complex $[\text{M}_2]\text{L}$, the minor isomer of II present in solution at -20°C , also reacts with excess PMe_3 to give $[\text{M}_2]\text{L}_2$, as demanded by eq 5.

Solution Behavior of I + dmpm and III. The addition of dmpm to a toluene- d_8 solution of I at -78°C give ^{31}P and ^1H NMR spectra consistent with the formation of III, an analogue of the symmetrical bisphosphine compound $[\text{M}_2]\text{L}_2$, described in the previous section. Upon warming the sample to room temperature the ^1H and ^{31}P spectra are indicative of the formation of a monoligated complex $(\eta^1\text{-dmpm})(\text{PhCH}_2)_2(i\text{-PrO})\text{Mo}\equiv\text{Mo}(\text{O-}i\text{-Pr})_3$. The specific evidence for the 1,1-dibenzyl groups arises from the methylene protons of the CH_2Ph ligands which appear as an ABX spin system. Moreover, the *O-i-Pr* ligands show a 3:1 grouping as was seen for II in the temperature range 0 to $+22^\circ\text{C}$.

When the temperature is lowered, the ^1H and ^{31}P spectra reveal that III is reformed but that another complex is present in roughly equal concentration. We propose that this is $(\eta^2\text{-}\mu\text{-dmpm})\text{Mo}_2(\text{CH}_2\text{Ph})_2(\text{O-}i\text{-Pr})_4$ that contains the 1,1 arrangement of benzyl ligands. Compound III can be crystallized from solutions at -5°C at which temperature the $\eta^1\text{-dmpm}$ ligand undergoes rapid exchange of its bonded and terminal PMe_2 groups. Evidently, the benzyl/alkoxide migration is facile in the temperature range 0 to $+22^\circ\text{C}$.

Solution Behavior of $\text{Mo}_2(\text{CH}_2\text{Ph})_2(\text{O-}i\text{-Pr})_4(\text{dmpe})$ (IV). Compound IV is essentially insoluble in hydrocarbon solvents and sparingly soluble in THF. However, in the presence of a second equivalent of dmpe and under photolysis, compound IV reacts to give the known com-

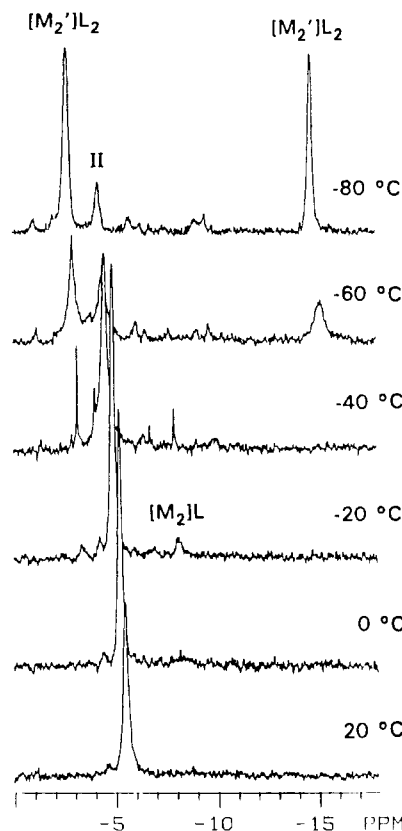


Figure 7. $^{31}\text{P}\{^1\text{H}\}$ NMR spectra showing the temperature-dependent equilibrium of II and $[\text{M}_2']$ in the presence of PMe_3 (2.5 equiv).

pound (*i*-PrO) $_4\text{Mo}\equiv\text{Mo}(\text{dmpe})_2$ ¹² with the elimination of bibenzyl.

Concluding Remarks. This work provides the first example of the observation of the facile reversible migration of ligands across a $\text{Mo}\equiv\text{Mo}$ bond in the chemistry of $\text{Mo}_2\text{X}_2\text{Y}_4$ compounds. This type of migration is of potential importance to a wide variety of reactions at these dinuclear centers.

Previously, we have found that the 1,1- and 1,2-isomers of formula $\text{M}_2\text{X}_2\text{Y}_4$ (e.g. $\text{M} = \text{Mo}$, $\text{X} = \text{NMe}_2$ or *O*-*t*-Bu, $\text{Y} = \text{CH}_2\text{SiMe}_3$) do not isomerize in solution even at +80 °C over a period of 1 h.¹³ Bridge formation for d^3 - d^3 $\text{XY}_2\text{M}\equiv\text{MY}_2\text{X}$ compounds is not favored because it greatly weakens metal-metal bonding. The M-M bonding for a d^3 - d^3 bitetrahedron yields a M-M single bond of configuration $\sigma^2(\delta\delta^*)^4$. When metal-ligand multiple bonding can be maximized, the enthalpy gained in forming a metal-ligand bridge is very small, if indeed favorable. Only in the case of bisphosphido complexes of formula $\text{W}_2(\text{PR}_2)_2(\text{NMe}_2)_4$ have we seen the existence of bridged isomers $\text{W}_2(\mu\text{-PR}_2)_2(\text{NMe}_2)_4$.¹⁴ In the bridged isomers, the W-P distances are slightly shorter than those of the terminal W-PR₃ ligands in the unbridged isomers. Evidently, the loss of W-W bonding in going from the ethane-like geometry is compensated for by the formation of two additional strong W-P bonds. The rate of phosphido bridge opening and closing is quite slow, however, since the ΔG^\ddagger values are about 24 kcal mol⁻¹ at 25 °C.¹⁴ For these reasons we discount the possibility that the

Table IV. Fractional Coordinates and Isotropic Thermal Parameters for the $\text{Mo}_2(\text{CH}_2\text{Ph})_2(\text{O-}i\text{-Pr})_4(\text{PMe}_3)$ Molecules

atom	10 ⁴ x	10 ⁴ y	10 ⁴ z	<i>B</i> _{iso} (Å ²)
Mo(1)	2739.8 (3)	723.9 (4)	1175.2 (2)	20
Mo(2)	1712.4 (3)	1829.1 (5)	1616.8 (2)	22
P(3)	2154 (1)	-1585 (1)	1427 (1)	19
C(4)	1975 (4)	-2039 (6)	2314 (3)	30
C(5)	2767 (3)	-2965 (5)	1148 (3)	24
C(6)	1206 (3)	-2033 (6)	1024 (3)	26
O(7)	3475 (2)	2031 (9)	851 (2)	32
C(8)	3541 (4)	3444 (5)	848 (3)	30
C(9)	4182 (4)	3860 (6)	1339 (3)	31
C(10)	3716 (5)	3896 (7)	133 (4)	45
C(11)	3414 (3)	137 (6)	2106 (3)	28
C(12)	4061 (3)	-825 (5)	1974 (3)	21
C(13)	4170 (3)	-1974 (6)	2362 (3)	26
C(14)	4752 (3)	-2891 (6)	2211 (3)	27
C(15)	5251 (3)	-2704 (6)	1670 (3)	28
C(16)	5182 (3)	-1560 (6)	1291 (3)	29
C(17)	4591 (3)	-635 (5)	1448 (3)	26
C(18)	2234 (3)	142 (5)	167 (3)	25
C(19)	2699 (3)	-891 (5)	-209 (3)	26
C(20)	2321 (4)	-1924 (6)	-552 (3)	28
C(21)	2755 (4)	-2929 (6)	-851 (3)	33
C(22)	3573 (4)	-2907 (6)	-836 (3)	35
C(23)	3946 (4)	-1870 (6)	-520 (3)	36
C(24)	3522 (4)	-872 (6)	-212 (3)	29
O(25)	979 (2)	502 (4)	1909 (2)	32
C(26)	222 (4)	927 (7)	2174 (4)	40
C(27)	-402 (5)	715 (16)	1623 (6)	106
C(28)	86 (6)	205 (11)	2800 (6)	90
O(29)	1290 (2)	2905 (4)	917 (2)	30
C(30)	1310 (3)	3201 (6)	210 (3)	28
C(31)	602 (4)	2545 (6)	-138 (4)	39
C(32)	1271 (4)	4691 (6)	113 (4)	40
O(33)	2080 (3)	2871 (4)	2348 (2)	39
C(34)	2694 (4)	3175 (6)	2815 (3)	34
C(35)	2800 (4)	4655 (6)	2860 (3)	32
C(36)	2489 (5)	2588 (8)	3500 (3)	47

1,2- $\text{Mo}_2(\text{CH}_2\text{Ph})_2(\text{O-}i\text{-Pr})_4$ compound, I, exists in solution at temperatures above 0 °C in a chemically rapid equilibrium with its 1,1-dibenzyl isomer.

We propose that the initially formed monophosphine adduct is formed rapidly and reversibly by addition of PMe_3 to I. In the ground state this is structurally similar to 1,2- $\text{W}_2(\text{Ar})_2(\text{O-}i\text{-Pr})_4(\text{HNMe}_2)$, but isomerization to the 1,1-isomer, compound II, is kinetically facile by way of a bridged intermediate. It is interesting to speculate about the possible structure of a bridged intermediate. In a formal sense it is a bridged d^3 - d^3 M_2L_7 complex and could have a M_2L_7 unit similar to the W_2Cl_7 unit found in the structure of the $\text{W}_2\text{Cl}_7(\text{THF})_2^-$ anion.¹⁵ Note that a con-facial bioctahedron the d^3 - d^3 interaction forms a $\sigma^2\pi^4$ M-M triple bond. A triply bridging M_2L_7 molecule may be viewed as a derivative of the $\text{X}_3\text{M}(\mu\text{-X})_3\text{MX}_3$ structure by the removal of two terminal ligands, and as such would retain the essential features of the M-M bonding. It is for this reason that we believe the addition of PMe_3 promotes or facilitates the migration of the benzyl/alkoxide ligands. It is not clear why the PMe_3 adduct of the 1,1-dibenzyl isomer is favored over that of the 1,2-isomer. They are, however, in a 3:1 equilibrium at -20 °C so the energy difference is very small. Moreover, the energy of the bridged species cannot be more than ca. 15 kcal mol⁻¹ higher than that of the unbridged isomers or they would not rapidly interconvert at 0 °C.

On the basis of the present findings, we propose that addition of X^- to $\text{M}_2(\text{OR})_6$ compounds will yield bridged

(12) Chisholm, M. H.; Huffman, J. C.; Van Der Sluys, W. G. *J. Am. Chem. Soc.* 1987, 109, 2514.

(13) Chisholm, M. H.; Folting, K.; Huffman, J. C.; Rothwell, I. P. *Organometallics* 1982, 1, 251.

(14) Buhro, W. E.; Chisholm, M. H.; Martin, J. D.; Folting, K.; Huffman, J. C.; Streib, W. E. *J. Am. Chem. Soc.* 1992, 114, 557.

(15) (a) Chisholm, M. H.; Eichhorn, B. W.; Folting, K.; Huffman, J. C.; Ontiveros, C. D.; Streib, W. E.; Van Der Sluys, W. G. *Inorg. Chem.* 1987, 26, 3182. (b) Bergs, D. J.; Chisholm, M. H.; Folting, K.; Huffman, J. C.; Stahl, K. A. *Inorg. Chem.* 1988, 27, 2950.

Table V. Fractional Coordinates and Isotropic Thermal Parameters for the $\text{Mo}_2(\text{CH}_2\text{Ph})_2(\text{O}-i\text{-Pr})_4(\text{dppm})$ Molecule

atom	10^4x	10^4y	10^4z	B_{iso} (\AA^2)	atom	10^4x	10^4y	10^4z	B_{iso} (\AA^2)
Mo(1)A	2773 (1)	9906.0 (3)	2146.8 (5)	18	Mo(1)B	7393 (1)	12384.9 (3)	2949.7 (5)	16
Mo(2)A	2140 (1)	9838.6 (3)	3124.5 (4)	18	Mo(2)B	8044 (1)	12356.5 (3)	1980.4 (5)	19
P(3)A	1250 (2)	10594 (1)	2665 (2)	25	P(3)B	8820 (2)	13140 (1)	2454 (2)	27
C(4)A	2173 (8)	11019 (4)	2699 (6)	34	C(4)B	7835 (7)	13531 (4)	2416 (7)	35
P(5)A	3253 (2)	10749 (1)	2638 (2)	29	P(5)B	6784	13206 (1)	2460 (2)	29
C(6)A	666 (9)	10842 (4)	3327 (7)	41	C(6)B	9376 (8)	13432 (4)	1825 (7)	39
C(7)A	313 (7)	10663 (3)	1686 (7)	30	C(7)B	9754 (7)	13233 (4)	3447 (7)	33
C(8)A	4201 (8)	10900 (4)	3595 (6)	39	C(8)B	5836 (8)	13330 (4)	1496 (7)	45
C(9)A	3583 (9)	11142 (4)	1973 (6)	43	C(9)B	6396 (8)	13564 (4)	3139 (8)	43
C(10)A	697 (6)	9571 (3)	2424 (6)	22	C(10)B	9520 (6)	12130 (3)	2715 (6)	22
C(11)A	49 (6)	9626 (3)	2904 (6)	20	C(11)B	10147 (6)	12134 (3)	2221 (5)	22
C(12)A	-883 (6)	9802 (3)	2545 (6)	23	C(12)B	11038 (7)	12366 (4)	2495 (6)	30
C(13)A	-1472 (8)	9875 (4)	2986 (8)	37	C(13)B	11620 (7)	12370 (4)	2034 (7)	39
C(14)A	-1116 (9)	9775 (4)	3814 (8)	45	C(14)B	11338 (7)	12152 (4)	1286 (7)	33
C(15)A	-215 (9)	9586 (3)	4170 (7)	39	C(15)B	10475 (7)	11920 (3)	1002 (6)	26
C(16)A	361 (7)	9515 (3)	3719 (6)	23	C(16)B	9894 (6)	11907 (3)	1474 (6)	23
C(17)A	4286 (6)	9766 (4)	2858 (6)	30	C(17)B	5882 (7)	12218 (4)	2258 (6)	27
C(18)A	4802 (7)	9837 (6)	2297 (6)	28	C(18)B	5355 (6)	12314 (5)	2800 (6)	21
C(19)A	4711 (7)	9542 (4)	1662 (7)	30	C(19)B	5617 (7)	12180 (4)	3575 (6)	29
C(20)A	5160 (7)	9607 (4)	1108 (7)	33	C(20)B	5181 (7)	12233 (4)	4105 (6)	33
C(21)A	5710 (7)	9986 (4)	1157 (6)	35	C(21)B	4474 (7)	12564 (4)	3904 (7)	39
C(22)A	5846 (8)	10283 (4)	1781 (7)	41	C(22)B	4213 (7)	12763 (4)	3150 (6)	34
C(23)A	5383 (7)	10211 (4)	2337 (6)	38	C(23)B	4640 (7)	12638 (4)	2608 (6)	31
O(24)A	2545 (4)	9259 (9)	3651 (3)	22	O(24)B	7744 (4)	11768 (2)	1464 (4)	22
C(25)A	3118 (7)	8869 (3)	3709 (6)	27	C(25)B	7137 (7)	11377 (4)	1363 (6)	26
C(26)A	4033 (7)	8921 (4)	4430 (6)	36	C(26)B	6271 (9)	11441 (5)	619 (7)	53
C(27)A	2566 (8)	8458 (4)	3792 (7)	34	C(27)B	7734 (8)	10972 (4)	1318 (8)	42
O(28)A	2847 (9)	10265 (2)	3995 (4)	30	O(28)B	7287 (4)	12768 (2)	1108 (4)	29
C(29)A	2681 (8)	10286 (4)	4748 (6)	33	C(29)B	7366 (9)	12911 (7)	384 (9)	68
C(30)A	2993 (11)	10751 (4)	5129 (7)	58	C(30)B	7990 (17)	12685 (6)	242 (9)	97
C(31)A	3223 (8)	9905 (5)	5299 (6)	41	C(31)B	6570 (21)	12981 (9)	-243 (9)	178
O(32)A	1928 (4)	10283 (2)	1251 (3)	22	O(32)B	8187 (4)	12784 (2)	3847 (4)	25
C(33)A	2163 (9)	10384 (4)	540 (6)	37	C(33)B	7980 (7)	12856 (4)	4559 (6)	33
C(34)A	1560 (9)	10753 (5)	106 (7)	51	C(34)B	8520 (8)	13283 (4)	4972 (8)	49
C(35)A	2123 (11)	9958 (6)	24 (8)	65	C(35)B	8296 (8)	12451 (4)	5119 (6)	40
O(36)A	2617 (4)	9319 (2)	1640 (3)	19	O(36)B	7624 (4)	11801 (2)	3469 (4)	20
C(37)A	2119 (6)	8901 (3)	1554 (6)	22	C(37)B	8126 (8)	11388 (3)	3562 (6)	29
C(38)A	1196 (7)	8923 (4)	801 (6)	30	C(38)B	9031 (9)	11414 (4)	4287 (7)	46
C(39)A	2751 (8)	8517 (4)	1482 (6)	33	C(39)B	7456 (11)	11003 (4)	3603 (9)	53

complexes $\text{M}_2(\text{X})(\text{OR})_6^-$ when X = halide, alkoxide, siloxide, thiolate, etc. The bridge species will be favored by internal charge compensation in the anion. This contrasts with the unbridged compounds of formula $\text{M}_2(\text{OR})_6\text{L}_2$, which contain weak and labile M-L bonds (L = amine, pyridine, or tertiary phosphine) and retain the essential elements of the ethane-like $\text{M}_2(\text{OR})_6$ parent complexes.

Further work aimed at testing this hypothesis is planned.

Experimental Section

General Procedures. All syntheses and sample manipulations were carried out under an atmosphere of dry and oxygen-free nitrogen using standard Schlenk and glovebox techniques. Hydrocarbon solvents were distilled under N_2 from Na/benzophenone and stored over 4-Å molecular sieves. ^1H NMR spectra were recorded on a Varian XL-300 spectrometer at 300 MHz in dry and deoxygenated benzene- d_6 or toluene- d_8 . ^{31}P NMR spectra were recorded on a Nicolet NT-360 spectrometer at 146 MHz in the same solvents. All ^1H NMR chemical shifts are reported in ppm relative to the residual protio impurities of the deuterated solvents. ^{31}P NMR chemical shifts are reported in ppm relative to an external 85% H_3PO_4 standard set at 0.0 ppm. Infrared spectra were obtained from KBr pellets using a Nicolet S10P FT-IR spectrometer. Elemental analyses were performed by Oneida Research Services.

Chemicals. $\text{Mo}_2(\text{CH}_2\text{Ph})_2(\text{O}-i\text{-Pr})_4$ ¹⁶ and PMe_3 ¹⁷ were synthesized according to previously published procedures. Dmpm and dmpe were purchased commercially and used as received.

$\text{Mo}_2(\text{CH}_2\text{Ph})_2(\text{O}-i\text{-Pr})_4(\text{PMe}_3)$ (II). $\text{Mo}_2(\text{CH}_2\text{Ph})_2(\text{O}-i\text{-Pr})_4$ (0.200 g, 0.328 mmol) was dissolved in hexane (5 mL). PMe_3 (0.064 mL, 0.655 mmol) was then added by syringe. The mixture was cooled to -25°C . After 2 days orange crystals were isolated and dried in vacuo (yield: 0.165 g, 73%). ^1H NMR (-5°C , toluene- d_8): δ 6.03 (br m, 1 H, $\text{OCH}(\text{CH}_3)_2$), 4.70 (m, 3 H, $J = 6.0$ Hz, $\text{OCH}(\text{CH}_3)_2$), 4.54 (ABX (X = ^{31}P), 4 H, CH_2Ph), 1.82 (d, 6 H, $J = 6.3$ Hz, $\text{OCH}(\text{CH}_3)_2$), 1.30 (d, 18 H, $J = 6.0$ Hz, $\text{OCH}(\text{CH}_3)_2$), 0.957 (d, 9 H, $J_{\text{HP}} = 7.8$ Hz, PMe_3). $^{31}\text{P}\{^1\text{H}\}$ NMR (20 $^\circ\text{C}$, toluene- d_8): δ -5.61 (br s, PMe_3). IR (KBr pellet, cm^{-1}): 2965 (m), 2921 (w), 2861 (w), 1593 (m), 1487 (m), 1375 (m), 1362 (m), 1325 (m), 1206 (w), 1164 (m), 1111 (s), 986 (s), 955 (s), 843 (m), 828 (m), 749 (s), 698 (m), 654 (w), 610 (w), 586 (w).

$\text{Mo}_2(\text{CH}_2\text{Ph})_2(\text{O}-i\text{-Pr})_4(\text{dmpm})$ (III). $\text{Mo}_2(\text{CH}_2\text{Ph})_2(\text{O}-i\text{-Pr})_4$ (0.150 g, 0.247 mmol) was dissolved in hexane (10 mL). Dmpm (0.270 mmol, 0.073 g) was then added via microliter syringe. The mixture was warmed gently to redissolve a small amount of precipitate which began forming. Cooling to -5°C and then to -25°C gave two crops of crystals (total yield: 0.160 g, 87%). Anal. Calcd for $\text{Mo}_2\text{C}_{31}\text{H}_{56}\text{P}_2\text{O}_4$: C, 49.87; H, 7.56. Found: C, 49.72; H, 7.85. ^1H NMR (22 $^\circ\text{C}$, toluene- d_8): δ 5.87 (br m, 1 H, $\text{OCH}(\text{CH}_3)_2$), 5.00 (br m, 3 H, $\text{OCH}(\text{CH}_3)_2$), 4.40 (ABX (X = ^{31}P), 4 H, CH_2Ph), 2.32 (t, 2 H, $J_{\text{HP}} = 9$ Hz, $\text{Me}_2\text{PCH}_2\text{PMe}_2$), 1.77 (d, 3 H, $J = 5.4$ Hz, $\text{OCH}(\text{CH}_3)_2$), 1.34 (d, 9 H, $J = 6.0$ Hz, $\text{OCH}(\text{CH}_3)_2$), 1.15 (d, 6 H, $J_{\text{HP}} = 6.0$ Hz, $(\text{CH}_3)_2\text{PCH}_2\text{P}(\text{CH}_3)_2$), 0.99 (d, 6 H, $J_{\text{HP}} = 7.8$ Hz, $(\text{CH}_3)_2\text{PCH}_2\text{P}(\text{CH}_3)_2$). $^{31}\text{P}\{^1\text{H}\}$ NMR (-20°C , toluene- d_8): δ = -7.42 (s, 2 P, $\text{Me}_2\text{PCH}_2\text{PMe}_2$). IR (KBr pellet, cm^{-1}): 2961 (s), 2913 (m), 1593 (m), 1485 (m), 1372 (m), 1358 (m), 1321 (m), 1293 (w), 1277 (w), 1200 (w), 1157 (m), 1121 (s), 1030 (w), 990 (s), 951 (s), 843 (m), 747 (m), 700 (m), 583 (m), 448 (s).

$\text{Mo}_2(\text{CH}_2\text{Ph})_2(\text{O}-i\text{-Pr})_4(\text{dmpe})$ (IV). $\text{Mo}_2(\text{CH}_2\text{Ph})_2(\text{O}-i\text{-Pr})_4$ (0.150 g, 0.246 mmol) was dissolved in hexane (50 mL). Dmpe (0.041 g, 0.270 mmol) was added via syringe. The mixture was swirled once and left to stand at room temperature. Within minutes red microcrystals began to form. After 6 h the solvent

(16) Chisholm, M. H.; Tatz, R. J. *Organometallics* 1986, 5, 1590.

(17) Luetkens, M. L.; Sattelberger, A. P.; Murray, H. H.; Basil, J. D.; Fackler, J. P., Jr. *Inorg. Synth.* 1990, 28, 305.

was removed and the crystals were washed with 10 mL of hexane (yield: 0.175 g, 94%). Anal. Calcd for $\text{Mo}_2\text{P}_2\text{O}_4\text{C}_{32}\text{H}_{58}$: C, 50.53; H, 7.69. Found: C, 51.34; H, 7.66. IR (KBr pellet, cm^{-1}): 2961 (s), 2915 (m), 2863 (m), 1593 (m), 1485 (m), 1449 (w), 1372 (m), 1356 (m), 1321 (m), 1200 (m), 1157 (m), 1119 (s), 994 (s), 955 (s), 830 (m), 793 (w), 745 (m), 762 (m), 635 (s), 577 (m), 531 (w), 448 (w).

$\text{Mo}_2(\text{O}-i\text{-Pr})_4(\text{dmpe})_2$. Dmpe (0.104 g, 0.691 mmol) was added to a 20-mL THF solution of $\text{Mo}_2(\text{CH}_2\text{Ph})_2(\text{O}-i\text{-Pr})_4$ (0.250 g, 0.329 mmol) via syringe. The mixture was stirred at 22 °C under a UV lamp for 2 days. Solvent was removed in vacuo, and hexane was then added to the yellow-brown residue. Cooling to -25 °C yielded two crops of brown microcrystals (yield: 0.200 g, 83%) identified as $\text{Mo}_2(\text{O}-i\text{-Pr})_4(\text{dmpe})_2$ by ^1H and ^{31}P NMR spectroscopy.¹²

Crystallographic Studies. General operating procedures and listings of programs have been given previously.¹⁸ A summary of crystal data is given in Table I.

$\text{Mo}_2(\text{CH}_2\text{Ph})_2(\text{O}-i\text{-Pr})_4(\text{PMe}_3)$ (II). Large well-shaped crystals were present in the submitted sample, and a suitable fragment was cleaved from a representative crystal. After mounting and transferring to the goniostat by using inert atmosphere handling techniques, the crystal was characterized by a reciprocal lattice search technique. A set of diffraction maxima were located which could be indexed as monoclinic, space group $P2_1/c$.

The structure was solved by direct methods (MULTAN78) and Fourier techniques, and refined by full-matrix least squares. All hydrogen atoms were located and refined, although several were poorly behaved. A final difference Fourier was featureless, the largest peak being 0.59 $\text{e}/\text{\AA}^3$. No absorption correction was performed.

$\text{Mo}_2(\text{CH}_2\text{Ph})_2(\text{O}-i\text{-Pr})_4(\text{dmpm})$ (III). A suitable crystal was selected and transferred to the goniostat using inert atmosphere

handling techniques. The crystal was cooled to -168 °C for characterization and data collection.

A systematic search of a limited hemisphere of reciprocal space yielded a set of reflections exhibiting monoclinic symmetry ($2/m$). The systematic extinctions of $0k0$ for $k = 2n + 1$ and of $h0l$ for $h + l = 2n + 1$ uniquely identified the space group as $P2_1/n$. This choice was confirmed by the subsequent solution and refinement of the structure.

The structure was solved by the combination of direct methods (MULTAN) and Fourier techniques. All non-hydrogen atoms were located without difficulty; some of the hydrogen atoms were locatable in a later difference map. All hydrogen atoms were therefore calculated using idealized geometries and a C-H distance at 0.95 Å, they were assigned a fixed B of 1.0 Å² plus the isotropic equivalent of the parent atom. The full-matrix least-squares refinement of the structure was completed using anisotropic thermal parameters on all non-hydrogen atoms and fixed hydrogen atoms. Due to the large number of variables (704 total), the refinement was carried out in a cyclical manner. The final R was 0.056; $R_w(F)$ was 0.056.

The asymmetric unit contains two complete molecules, they are labeled A and B, respectively.

The final difference Fourier was essentially featureless, the largest peak was 2 $\text{e}/\text{\AA}$ in the vicinity of C(30)B, indicating a slight disorder in the isopropyl group. No attempts were made at modeling the disorder.

Atomic coordinates for compounds II and III are listed in Tables IV and V, respectively.

Acknowledgment. We thank the National Science Foundation for support.

Supplementary Material Available: Listings of anisotropic thermal parameters and bond distances and angles and VER-SORT stereodrawings (12 pages). Ordering information is given on any current masthead page.

OM920242A

(18) Chisholm, M. H.; Folting, K.; Huffman, J. C.; Kirkpatrick, C. C. *Inorg. Chem.* 1984, 23, 1021.

Agostic Assistance to Olefin Insertion in Alkylzirconocene Cations: A Molecular Orbital Study by the Extended Hückel Method

Marc-Heinrich Prosenç,[†] Christoph Janiak,[‡] and Hans-Herbert Brintzinger^{*†}

Fakultät für Chemie, Universität Konstanz, D-7750 Konstanz, Germany, and Kunststofflaboratorium, BASF AG, D-6700 Ludwigshafen, Germany

Received June 9, 1992

Alternative reaction modes for α -olefin insertion in a zirconocene alkyl cation are investigated by the extended Hückel MO method. Agostic interaction of one of the α -H atoms of the migrating alkyl group with the Zr center is found to stabilize the transition state of the preferred reaction mode. Essential contributions to this preference are identified by fragment-MO analysis. Implications of these findings for stereoselective olefin polymerization by chiral *ansa*-metallocene derivatives are discussed.

Introduction

Observations that homogeneous, metallocene-based catalyst systems can induce a stereospecific polymerization of α -olefins¹⁻³ have opened new possibilities to study the mechanisms of this catalysis, especially the origins of its

stereospecificity.⁴ Recently, we have reported that olefin insertion into α -deuterated alkyl derivatives of a zirconocene-based polymerization catalyst is influenced in its stereochemistry by kinetic isotope effects.⁵ Piers and

* Author to whom correspondence should be addressed.

[†] Universität Konstanz.

[‡] BASF AG. Present address: Institut für Anorganische und Analytische Chemie, Technische Universität Berlin, D-1000 Berlin 12, Germany.

(1) Ewen, J. A. *J. Am. Chem. Soc.* 1984, 106, 6355-6364.

(2) Kaminsky, W.; Külper, K.; Brintzinger, H. H.; Wild, F. R. W. P. *Angew. Chem., Int. Ed. Engl.* 1985, 24, 507-508.

(3) Reviews: Krentsel, B. A.; Nekhaeva, L. A. *Russ. Chem. Rev.* 1990, 59, 1193-1207. Skupinska, J. *Chem. Rev.* 1991, 91, 613-648.

(4) Pino, P.; Cioni, P.; Wei, J. *J. Am. Chem. Soc.* 1987, 109, 6189-6191.

(5) Krauledat, H.; Brintzinger, H. H. *Angew. Chem., Int. Ed. Engl.* 1990, 29, 1412-1413.